Mechanisms of ovipositor insertion and steering of a parasitic wasp

Uroš Cerkvenik[a,1], Bram van de Straat[a], Sander W. S. Gussekloo[a], and Johan L. van Leeuwen[a]

[a]Experimental Zoology Group, Wageningen University and Research, 6708WD Wageningen, The Netherlands

Edited by Raghavendra Gadagkar, Indian Institute of Science, Bangalore, India, and approved July 28, 2017 (received for review April 13, 2017)

Drilling into solid substrates with slender beam-like structures is a mechanical challenge, but is regularly done by female parasitic wasps. The wasp inserts her ovipositor into solid substrates to deposit eggs in hosts, and even seems capable of steering the ovipositor while drilling. The ovipositor generally consists of three longitudinally connected valves that can slide along each other. Alternative valve movements have been hypothesized to be involved in ovipositor damage avoidance and steering during drilling. However, none of the hypotheses have been tested in vivo. We used 3D and 2D motion analysis to quantify the probing behavior of the fruit-fly parasitoid *Diachasmimorpha longicaudata* (Braconidae) at the levels of the ovipositor and its individual valves. We show that the wasps can steer and curve their ovipositors in any direction relative to their body axis. In a soft substrate, the ovipositors can be inserted without reciprocal motion of the valves. In a stiff substrate, such motions were always observed. This is in agreement with the damage avoidance hypothesis of insertion, as they presumably limit the overall net pushing force. Steering can be achieved by varying the asymmetry of the distal part of the ovipositor by protracting one valve set with respect to the other. Tip asymmetry is enhanced by curving of ventral elements in the absence of an opposing force, possibly due to pretension. Our findings deepen the knowledge of the functioning and evolution of the ovipositor in hymenopterans and may help to improve man-made steerable probes.

Diachasmimorpha longicaudata | ovipositor kinematics | buckling avoidance | spatial probing | minimally invasive probe

From a mechanical perspective, it is very difficult to drill into a solid substrate with a very thin probe, because it can easily bend and break. Parasitic wasps, however, do this regularly when they use their slender ovipositors to search for hosts in solid substrates, such as fruits or even wood (1–3).

The general morphology of the ovipositor is similar across all wasp species (4, 5); it consists of four elements, called valves, of which two are often merged such that three functional valves remain (Fig. 1). In most species, the distal part of the ovipositor is morphologically distinct (3, 6), which we will refer to as the tip. The valves can slide along each other (5, 7) and do not get dislocated under natural conditions, because they are longitudinally connected via a tongue-and-groove mechanism (5, 8–10). The ovipositor and the "wasp waist," a constriction of the body between the first and second abdominal segment (11), are essential in probing behavior and are therefore considered to be instrumental in the evolution of the order (11–15). The shape, structure, and mechanical properties of the ovipositors are putatively adapted to the substrates into which the animals need to probe (6, 16–18), and because both substrates and hosts are so diverse, this might have resulted in high species diversification of the hymenopterans (13, 14). However, to understand the observed diversity in the ovipositor shapes, understanding of the probing mechanics is essential.

Wasps are faced with two problems when searching for hosts in (solid) substrates: (*i*) how to insert the ovipositor without buckling/breaking it and (*ii*) how to maneuver with the ovipositor to reach the target.

Buckling is a mechanical failure of a structure which occurs, for instance, when a beam cannot withstand the applied axial load and bends, possibly beyond its breaking point. As buckling occurs more easily in slender beams, this is a real danger for parasitic wasps. Buckling depends on four parameters: (*i*) the axial load applied on the beam, (*ii*) the second moment of area of the beam, (*iii*) how well is the beam fixed on both ends (i.e., "free to slide sideways," "hinged," or "fixed"), and (*iv*) the length of the beam.

During puncturing, axial loading of the ovipositor cannot be avoided, so only the other factors can be adjusted. The second moment of area is largely determined by the diameter of the ovipositor and its wall thickness. To simplify insertion, the ovipositor must be as thin as possible, while the internal channel needs to be big enough for an egg to pass. Both of these requirements increase the chance of buckling. In all wasps, the ovipositor is fixed internally to the reproductive system and the muscles that move the ovipositor (4, 19), so very little variance can be expected related to the fixation of the ovipositor. A parameter that can be changed is the "functional" length of the ovipositor. Some wasps protrude only a small part of the total ovipositor outside their bodies before puncturing the substrate. The part retained in the abdomen is then either strongly coiled or telescopically retracted (20, 21). In other species, the functional length of the ovipositor is reduced by supporting it by clamping the ovipositor with parts of their hind legs (11, 18, 22) or with specialized sheaths (1, 10, 23, 24).

Little is known about the mechanisms parasitic wasps use for further insertion and buckling prevention of the ovipositor after the initial puncturing of the substrate. Vincent and King (23) hypothesized a mechanism that wasps might use based on the

Significance

Using slender probes to drill through solids is challenging, but desirable, due to minimal disturbances of the substrate. Parasitic wasps drill into solid substrates and lay eggs in hosts hidden within using slender probes and are therefore a good model for studying mechanical challenges associated with this process. We show that wasps are able to probe in any direction with respect to their body orientation and use two methods of insertion. One of the methods implies a minimal net pushing force during drilling. Steering was achieved by adjusting the asymmetry of the probe's distal end. Knowledge on probing mechanisms of wasps is important for the understanding of the hymenopteran evolution and for the development of minimally invasive steerable probes.

Author contributions: U.C., S.W.S.G., and J.L.v.L. designed research; U.C. and B.v.d.S. performed experiments; U.C., B.v.d.S., S.W.S.G., and J.L.v.L. analyzed data; and U.C., S.W.S.G., and J.L.v.L. wrote the paper.

The authors declare no conflict of interest.

This article is a PNAS Direct Submission.

Data deposition: The data reported in this paper have been deposited in Dryad (doi.org/10.5061/dryad.8bc95).

[1]To whom correspondence should be addressed. Email: uros.cerkvenik@wur.nl.

This article contains supporting information online at www.pnas.org/lookup/suppl/doi:10.1073/pnas.1706162114/-/DCSupplemental.

www.pnas.org/cgi/doi/10.1073/pnas.1706162114

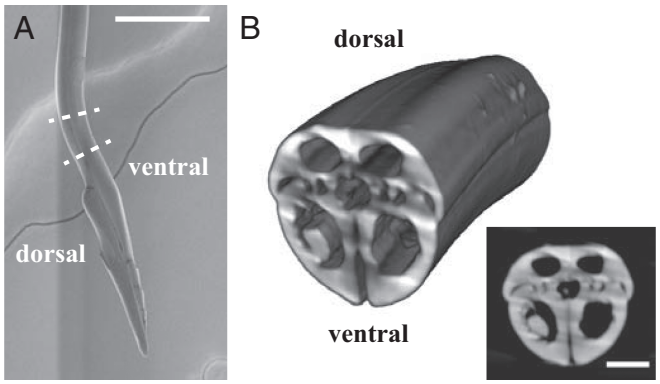

Fig. 1. Ovipositor of *D. longicaudata*. (*A*) SEM image of the ovipositor; side view. Region shown in *B* is indicated with dashed lines. (*B*) A 3D reconstruction of a part of the ovipositor obtained with a micro-CT scan. (*B*, *Inset*) Cross-section of the ovipositor showing the three valves. [Scale bar: 100 μm (*A*) and 10 μm (*B*, *Inset*)].

morphology of the ovipositor (Fig. 2*A*). In the proposed mechanism, wasps apply a pulling force on two of the three valves, which are kept stationary because of the hook-like structures on their tips function as anchors. These valves serve as guides for the third valve that is pushed inward. According to the hypothesis, buckling of the protracted valve is avoided by limiting the amplitudes of forward motion. By alternating the protraction and retraction of the valves, the ovipositor is further inserted into the substrate, while avoiding excessive net push forces and axial loads that could damage the ovipositor (23).

The second challenge during oviposition is that the wasps need to steer the ovipositor tip in the direction of the desired target (25). To do so, the ovipositor needs flexibility and a steering/bending mechanism that adjusts the tip direction during probing. Proposed bending mechanisms can be divided into passive and active ones (Fig. 2 *B–E*). Passive bending originates from mechanical interactions of the inserted ovipositor with the substrate. Active bending occurs when bending moments originate from the relative movements of the ovipositor valves.

Passive bending presumably occurs when an ovipositor has an asymmetric beveled tip (Fig. 2*B*). The asymmetric forces acting on such a tip push the tip away from a straight path (26, 27). Rotation of the bevel can be used to adjust the tip direction during insertion (28). The tips of most ovipositors across species are asymmetric (6, 29, 30) and can thus potentially function as a bevel. The bevel shape can presumably be enhanced by changing the relative positions of the valves. An adjustable bevel may control the degree of bending, similar to what has been proposed for a new generation of steerable needles (31).

Three mechanisms have been proposed for active bending. In the first mechanism, special anatomical structures limit the motion range of individual valves (32, 33). Bending occurs due to tension and compression in individual valves (Fig. 2*C*). A second active bending mechanism relies on differences in valve sclerotization (34). The distal part of ovipositors relying on this bending mechanism consists of heavily sclerotized, stiff arches, alternated with less sclerotized and flexible nodes. At rest, the arches and nodes of the dorsal and ventral valves are aligned and the ovipositor is approximately straight. When the ventral or dorsal valves are protracted, the arches align with nodes, which leads to bending (Fig. 2*D*). The third possible mechanism of active bending has been hypothesized for the control of hemipteran mouthparts. Similar to the ovipositors, the hemipteran mouthparts consist of multiple slender elements that are interconnected longitudinally and are able to slide along each other. It is assumed that bending moments in hemipteran mouthparts originate from (pre)tension of the elements (35, 36). The elements possess a certain level of inner tension and tend to curve to one side when not opposed. At rest, the elements are aligned with their tips so they counteract each other, resulting in a straight structure. When an individual element protracts, its tip curves inward toward the other elements (Fig. 2*E*). In all three mechanisms, the amplitude of the protraction and retraction of the valves probably correlates with the amount of bending and offers a way to control the curvature of the ovipositor during insertion.

Despite the proposed importance of ovipositors for the evolutionary success of hymenopterans, there is only a small number of empirical studies quantifying mechanical properties of the ovipositors (6, 16–18). The proposed theories of probing are based on morphological data, with only a few studies focusing on the ovipositor inside the substrate (25, 37), but no one has ever analyzed the dynamics of probing inside the substrate. In this work, we aim to quantify the ovipositor use (range, speed, and curvature of probing) in relation to substrate density and to determine which of the proposed methods of insertion and steering are used by parasitic wasps. We do this using the species *Diachasmimorpha longicaudata*, which provides an excellent example because of its long and slender ovipositor. Extrapolation of our results will also provide insight into probing and steering possibilities of other groups of parasitic hymenopterans and possibly of hemipterans and mosquitoes, as they use similar structures to probe for food. In addition, our study will add to the understanding of the functional demands acting on the ovipositor and the mechanism for drilling with slender probes. This, in turn, can be applied in the development of man-made instruments for tunneling, insertion, or probing. Such knowledge will presumably also help in the development of novel steerable surgical tools (38–43).

Results

We presented 28 wasps with two different gel densities and stiffnesses (parameters presented in Table 1 and Fig. S1). For details on calculations of gel parameters see *SI Materials and Methods*. Three wasps did not probe in both substrates. We analyzed only instances where wasps inserted >60% of their ovipositor inside

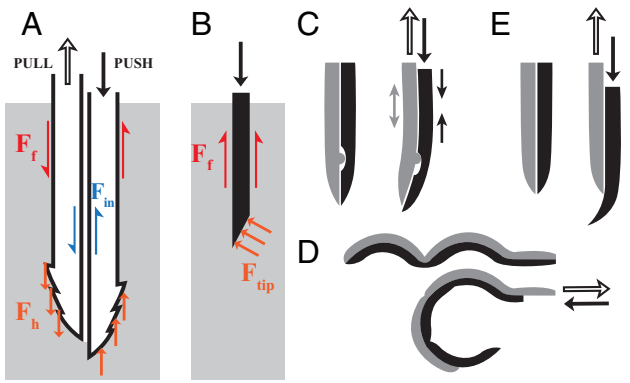

Fig. 2. Hypothesised insertion and steering mechanisms in 2D. Full arrows represent push forces and empty arrows pull forces. (*A*) The push–pull mechanisms (23) (only two valves are shown for clarity). Inner friction (F_{in}) is considered negligible. Friction along the shaft (F_f) of the two pulling valves, together with the hook forces (F_h), keep the ovipositor anchored in the substrate and counteract the friction and hook (cutting) forces of the pushing valve (modified from ref. 23). (*B*) A bevel shape of a needle leads to bending due to asymmetrical tip forces (F_{tip}). (*C*) Restriction in inter-element displacements (32) causes bending due to tensile (gray arrows) and compression (small black arrows) forces (modified from ref. 32). (*D*) Arched ovipositors bend due to differential sclerotization of valve segments (34); see text (modified from ref. 34). (*E*) Pretension of individual elements (35) leads to incurving upon their protraction as observed in hemipteran mouthparts (modified from ref. 35).

Table 1. Gel parameters. Storage (G′), loss (G″), dynamic shear (*G), and elastic (*E**) moduli**

Conc.	G′, kPa	G″, kPa	*G**, kPa	*E**, kPa
2%	11.970 ± 0.734	0.676 ± 0.278	11.989	35.967
4%	68.544 ± 2.016	4.615 ± 1.132	68.700	206.099

Conc., concentration.

the substrate. For three of the animals, the top camera recording their orientation during probing stopped working. Their data were excluded from the calculations of the range of probing, but were included in the velocity analysis. This amounted to 107 and 92 insertions used for range calculations, and 117 and 113 insertions for speed calculations in 2% and 4% gels, respectively.

Description of Probing Process. When starting to probe, an individual wasp lifted its abdomen, oriented the still-sheathed ovipositor vertically, and punctured the substrate with the most distal part of the ovipositor tip. While inserting the ovipositor deeper, the sheaths peeled away from the ovipositor base into a hairpin-like structure (Fig. 3*A*). Often, the wasp partially retracted the ovipositor within the substrate and reinserted it along a different trajectory. The wasp did not change its body orientation during an insertion session. A single insertion session contained 1–16 insertions (see Fig. 3*B* for a typical example of an insertion session). Individual insertions were not continuous, but consisted of minute retractions and reinsertions, especially when making curved insertions. The retractions were sometimes also used to make minor adjustments to the direction of insertion.

Probing Range. We calculated the maximum arc length of each insertion trajectory, as well as the radius (**r**), depth (**d**), and position vector (**R**) of the respective endpoints. We took the trajectory insertion angle α (deviation from 90°) as the angle between the **R** and the vertical vector along the depth axis (Fig. 3*B*).

From a single horizontal body orientation, wasps were able to probe in all directions within the gel (Fig. 3*C*), and we observed no directional preference of insertions belonging to the same session (Fig. S2). No clear directional preference was seen in the combined behavior of all animals (Rayleigh test, $P = 0.5$ and $P = 0.05$ for 2% and 4% gels, respectively).

The correlation between the vertical and horizontal component of the position vector (Pearson's correlation = 0.57, $P < 0.001$) shows that a deep probe had a large chance of having a limited horizontal amplitude and vice versa (Fig. 3*D*).

In general, the probing space of the wasps can be visualized as a cone with a curved base. The radius of the cone is substrate-dependent and is larger in the 2% gel than in the 4% gel (respective medians: 1.90 mm and 1.19 mm, Mann–Whitney *U* test, $P < 0.001$).

Deviation from a straight path of the insertion can be estimated by taking the ratio of its arc length and the magnitude of its **R**. Comparing the ratios against insertion angles, we see more insertions with high angles and with low bending in the 2% than in the 4% gel (Fig. 3*E*).

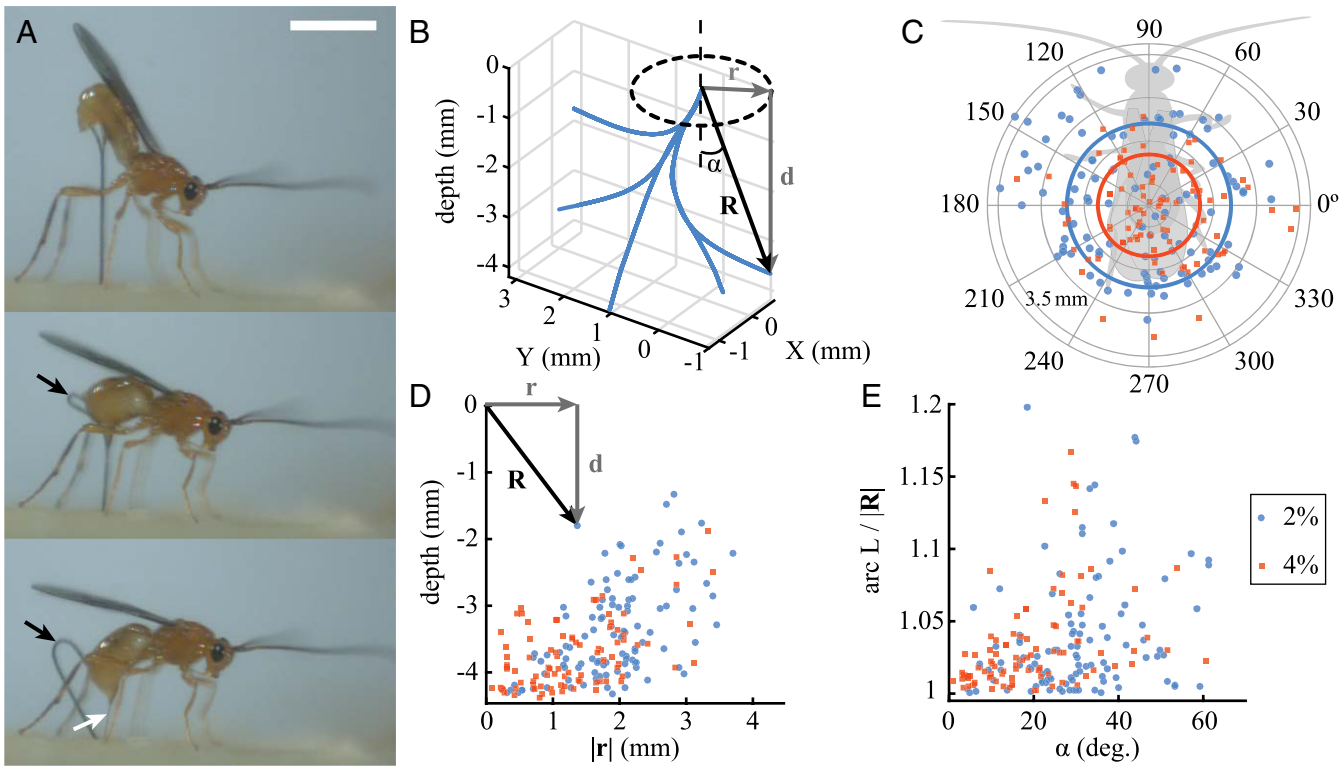

Fig. 3. Insertion behavior of probing wasps depends on substrate properties. (*A*) General probing behavior. The wasp positions its ovipositor vertically and punctures the substrate. The sheaths (black arrows) gradually detach and fold away from the ovipositor (white arrow) during deeper insertion. (Scale bar: 5 mm.) (*B*) Example of a single insertion session in 3D with parameters used in the analysis: **R**, position vector of the insertion trajectory endpoint; **r**, radius of the endpoint; **d**, depth vector; α, insertion angle. (*C*) Horizontal probing range showing the radii of the endpoints, corrected for the animal orientation (silhouette). Colored circles indicate median values of **r** for different substrates. Blue, 2% gel; red, 4% gel. (*D*) Vertical probing range: depth of trajectories plotted against their respective radii. The depth is shallower with increasing radius. (*E*) Ratio of arc length and the magnitude of **R** indicates the deviation from a straight path (ratio close to 1 indicates straight insertions). In softer gels, wasps reach higher radii by inserting their ovipositors straight, but at acute angles.

Curvature and Speed of Insertions. Wasps were able to strongly curve their ovipositors during probing with the maximal recorded values for curvature (κ) up to 1.6 mm^{-1}, or 0.048 dimensionless curvature (κ multiplied with the ovipositor width). Occasionally, we even captured complex insertion trajectories consisting of multiple bends in different directions. The majority of insertions, however, had very little curvature (Figs. 3*E* and 4). Most parts of insertions were <0.02 dimensionless curvature, with the median values 0.0060 and 0.0069 for 2% and 4% gel, respectively. Only ~1% of the parts of insertions had a dimensionless curvature >0.03. There was a slight, but significant, difference in curvature distribution between the 2% and 4% gels (Mann–Whitney U test, $P < 0.001$), and we observed more insertions with dimensionless curvatures >0.02 in the denser gel.

The ovipositor insertion was generally done at low speeds and accelerations (examples shown Figs. S3–S5). Wasps probed faster in 2% gel (Mann–Whitney U test, $P < 0.001$), with median insertion speed: 0.73 mm s^{-1} in 2% gel and 0.55 mm s^{-1} in 4% gel. There is also a clear relation between curvature and insertion speed (Fig. 4 and Fig. S6). Insertions with high curvature were always done at low speed. The highest speeds were only observed at low curvatures, although the majority of insertions, even with low curvature, were done at speeds <1.5 mm s^{-1}.

Changing Tip Morphology. We observed clear changes in the asymmetry of the ovipositor tip during relative movements of the dorsal and ventral valves (Fig. 5). When the dorsal valve was retracted, the ventral valve(s) curved dorsally across the midline of the ovipositor. When the ventral valves were retracted, however, no curving of the dorsal valve tip was observed. Protraction of ventral valves can be also seen in peaks of the tip orientation graphs (red arrows in Fig. 6).

Valve Kinematics and Steering. Wasps used two methods of ovipositor insertion, which are presented in the three examples in Fig. 6 (see also Movies S1–S3). In the first method, the ovipositor was pushed into the substrate as a whole, with very little relative movement of individual valves (pushing intervals noted in Fig. 6 *A* and *B*). This method was only observed in the softer, 2% substrate, and we will refer to this method as the "pushing method." The second, more common, method involved clear alternating movements of the valves throughout the insertion process, which we will call the "alternating method" (Fig. 6 *A* and *C*).

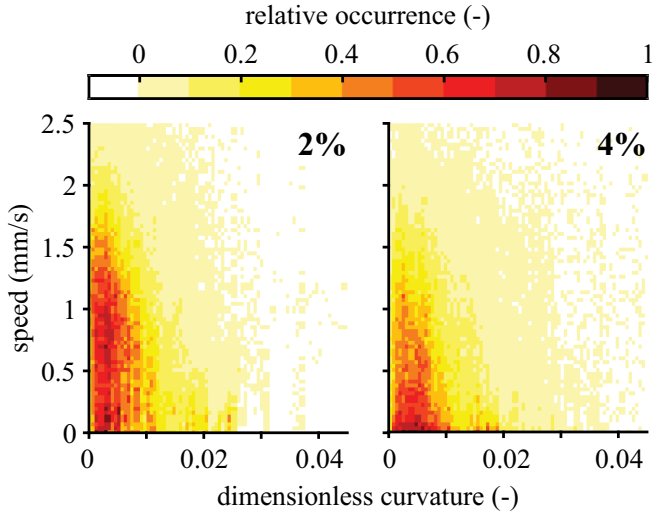

Fig. 4. Speed of probing decreases with increasing dimensionless curvature (κ multiplied with ovipositor diameter) and stiffness of the substrate. The heat maps show the relative frequency of specific speed and curvature combinations. Each axis has been divided into 80 bins of equal size, and the occurrence (number) of the points relative to the number of points in the most dense bin in the grid is presented as the color of the contours. The general pattern is hardly effected by the bin-size (Fig. S6).

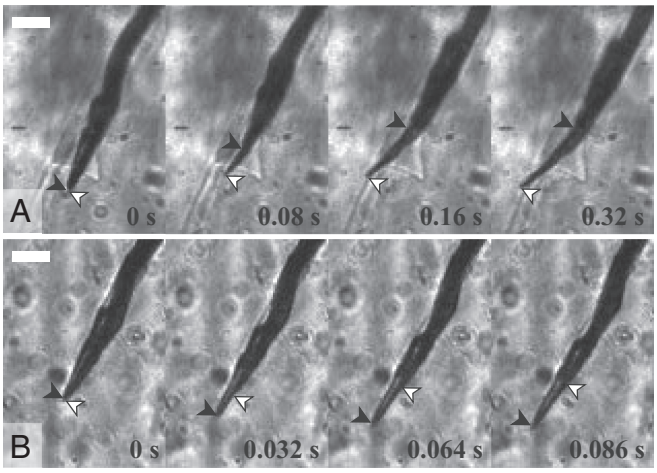

Fig. 5. Protraction of dorsal and ventral valves affect the shape of the ovipositor tip. (*A*) Protraction of the ventral valve(s) (white arrow) leads to the deformation and incuving of the ovipositor tip. (*B*) Protraction of the dorsal valve (black arrow) does not result in curving of the tip. (Scale bars: 50 μm.)

Straight and curved paths were achieved by using both of these methods. Straight insertions using the pushing method were obtained by inserting the ovipositors with valves aligned or a slight protraction of the dorsal valve. In the alternating method, the valves were moved around a positive offset value (Fig. 6*A* and Movie S1). Curved insertions were achieved by having the ventral valves protracted for an extended period. Minor changes in the negative valve offset were observed in the pushing method (Fig. 6*B* and Movie S2), whereas the valves moved around a negative offset value in the alternating method (Fig. 6*C* and Movie S3).

From the acceleration data, we calculated the net forces acting on the valves which were in the order of hundreds of piconewtons (*SI Materials and Methods* and Figs. S3–S5).

Discussion

Parasitic wasps probe into substrates to deposit eggs in hosts hidden within. Therefore, they need to pierce and explore the substrate (3, 6), locate the host, and sometimes also pierce through the host's integument (44–47), which is all done with the ovipositor apparatus only. Although the probing behavior of parasitic wasps has been repeatedly mentioned in the literature (3, 6, 17, 18, 48–51), no quantitative studies have been performed until now. Here, we show evidence that wasps are able to explore a large space from a single puncture point and that they use relative valve motions to insert and steer the ovipositor.

Movements of the ovipositor inside the substrate are complex and originate from the interplay between substrate and relative movements of individual ovipositor valves.

Two methods of ovipositor insertion were used by the wasps: (*i*) pushing of the entire ovipositor with minimal relative valve movements and (*ii*) insertions with alternating valve movements of high amplitude. During pushing, the valves were moved together, and the shape of the ovipositor tip barely changed. In the second method, the valves moved alternatively, resulting in a continuously changing shape of ovipositor tip.

The pushing method was only used in the soft gel, indicating that it might only be applicable in low-resistance environments. The second method, using alternating valve movements, was observed in both gels, showing that this can also be used

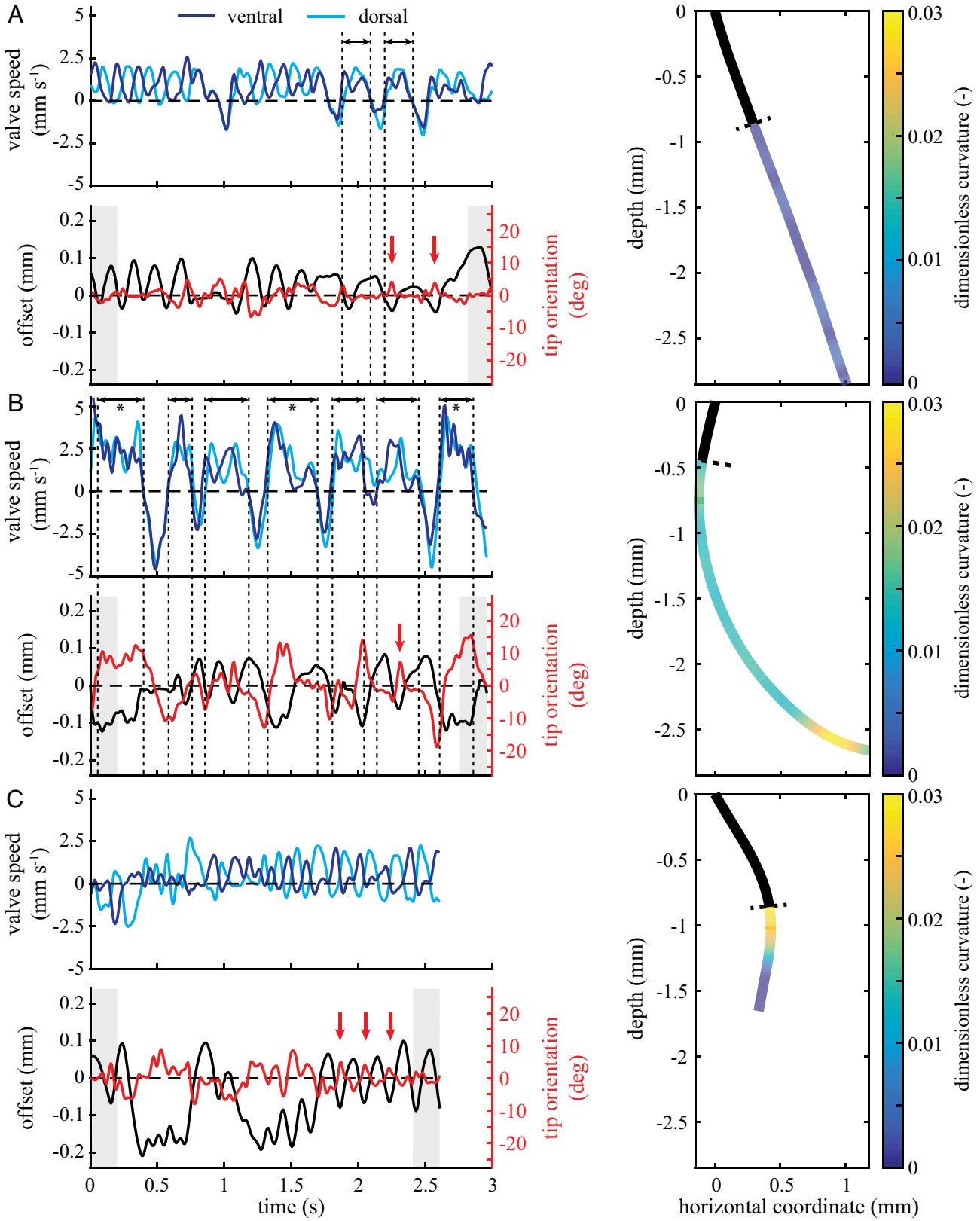

Fig. 6. Examples of ovipositor insertions. Shown are valve speeds, valve offset, tip orientation, and a 2D trajectory with its curvature (nontracked parts are shown in black). Shaded areas: less accurate calculations due to edge effects. Negative valve offset indicates protraction of dorsal valve(s). (*A*) Example of a straight insertion in 2% gel showing both methods of insertion: alternating valves (valve speed "out of phase") and pushing (valve speed "in phase"). Intervals above the graphs indicate the pushing method of ovipositor insertion (curving indicated with asterisks), and red arrows indicate the small changes in tip orientation that occur even on short protractions of the ventral valves (in all graphs). (*B*) Example of a curved insertion in 2% gel using the pushing method (intervals) with small changes in valve offset. (*C*) Example of a curved insertion in 4% gel using the alternating valve method. In both *B* and *C*, ventral valves are protracted for a prolonged period, which leads to sustained changes in tip orientation, resulting in a curved trajectory.

in high-resistance environments. This is in accordance with the mechanism proposed by Vincent and King (23), which predicts that alternating valve movement can be used for ovipositor insertion. According to the mechanism, some valves are being pulled at which anchors the ovipositor, allowing for the protraction of other valve(s). This predicted behavior is clearly seen in our data. Similar alternating movements, albeit of slender mouthparts (52), have also been reported in feeding mosquitoes. When probing in the host's integument, the mandibles and maxillae oscillate along their longitudinal axes (53–56).

Estimation of net forces on the valves (Figs. S3–S5) revealed that they are very low (piconewton range), which is also in agreement with the prediction of Vincent and King (23). Low forces were also suggested to occur during puncturing (55) and further insertion (57) of a mosquito proboscis. The low force values are partially attributed to the oscillatory movements of individual elements (55, 58). The forces estimated in this study are the sum of all forces acting on the ovipositor valves and can therefore not be directly compared with those in the mosquito experiments. The actual forces the valves exert on the substrate and friction forces within the substrate are probably substantially bigger. Unfortunately, it is currently not possible to obtain these forces in vivo. In addition, making accurate estimates of muscle forces is extremely difficult because of the small size of the animals. Our data nevertheless indicate that ovipositors can highly efficiently drill inside substrates, possibly with minimal net outside pushing force.

We observed that curved ovipositor trajectories were obtained using both insertion methods. The presence of multiple curves in single insertions indicates a degree of steering similar to that observed in previous studies on wasps (25, 37). Furthermore, the insertion trajectory pattern in a probing session (Fig. 2*B*) and the multiple bends within a single insertion are similar to what has been observed for the probing of hemipterans (35, 59, 60). This indicates that wasps and hemipterans might use similar mechanisms of probing. Both tend to explore a wide range of the susbtrate from a single puncture point. Several hypotheses have been postulated about the mechanism of ovipositor steering in wasps (5, 32, 33). Our direct observations of the probing process revealed that steering is achieved by shape changes of the ovipositor tip (Fig. 5), creating various degrees of geometrical asymmetry. This is similar to the bevelled tip of hypodermic needles, which has been shown to induce asymmetric reaction forces from the substrate that result in bending (27, 28, 61, 62). We observed three ways in which the wasp can create such an asymmetrical tip.

First, the morphology of the ovipositor tip is asymmetric (Fig. 1*A*), which might, by itself, result in bending effect, but this was rarely ($n = 2$) observed in our experiments. Second, by protracting one or more valves far beyond the other(s), the asymmetry of the tip is reinforced. This technique was observed during both insertion methods. In the third, most commonly observed, condition, the ventral valves are protracted to create a pronounced bevel. Protraction of the ventral valves (or retraction of the dorsal valve) caused the tip to bend toward the dorsal valve, probably because of the so-called preloading. Preloaded elements curved in a determined direction when no opposing force was present. The mechanism of preloaded elements has been proposed as a possible steering mechanism for hemipteran mouthparts (35). Although the incurving properties have been observed in mouthparts of dead hemipterans (36, 63, 64), they have never been observed in any species in vivo until now. Combining the second and the third point, one can expect that a bigger amplitude of ventral valve protraction will lead to stronger curvatures. This was, however, only partly confirmed in our study, as the amplitude of the negative offset does not always lead to a bigger change in tip orientation (Fig. 6). The inconsistency probably arises from the analysis of shadow images in which no distinction can be made between the two ventral valves, but which was necessary to increase the depth of focus of our recordings.

Our results show that wasps can explore a large volume by using the insertion and steering mechanisms described above. Furthermore, the wasp can do this from a single body orientation, using a single puncture point. Puncturing is arguably the most difficult step in probing, and it is therefore beneficial for the wasp if the ovipositor can be steered in any direction from a single puncture point. However, steering mechanisms described above only explain bending in one direction. Considering that the animal does not change the position of the body, the only other possible explanation for the observed range is that the animals are capable of rotating the ovipositor or its tip within the substrate.

For our species, the range can be envisioned similarly to a cone with the height equal to the length of the ovipositor and a curved base. The radius of the cone is dependent on the substrate stiffness and is slightly larger in the soft substrate. Despite a larger radius in the soft gel, the majority of insertions were still nearly straight, including insertions with a large horizontal displacement. This may be because the wasps inserted their ovipositors at acute angles with respect to the substrate surface. Unfortunately, it was impossible to determine the angle between the ovipositor and the substrate at the time of puncturing with our camera setup. Puncturing at acute angles is only possible when forces are small, because large lateral forces might result in buckling. In soft substrates, these forces are smaller than in stiff ones, allowing the wasps to puncture at shallow angles. However, such an angular insertion limits the possibility to probe in the opposite direction, because that would require very high curvatures.

In the stiff gel, there is a larger need to position the ovipositor perpendicular to the surface to avoid large lateral forces that might result in buckling. Therefore, in stiff substrates, wasps need to use bending of the ovipositor to enlarge their probing space. Our data show that this is achieved by adjusting the curvature for which relative movements of the valves are crucial. This is probably enhanced by the stronger reaction forces experienced as a result of the stiffer gel.

We also showed that substrate density has a negative effect on insertion speed. Stiffness (Fig. S1) and failure stress increase with gel density (65, 66), which makes penetration into denser substrates more energetically costly. The natural substrates the wasps probe into for hosts are, amongst others, citrus fruits, peaches, figs, and apples (67–69). It is impossbile to visualize the probing process in such substrates, so we substituted them for translucent gellan gels of different densities. There are some important differences between the gels and the fruits, as the latter are anisotropic and composed of layers and fibers. The shear and elastic moduli (Fig. S1) of the softest gel used in this study were approximately two orders of magnitude smaller than the moduli reported for mature peaches (70, 71) and the peel of citrus fruits (72, 73). The densest gel was only one order of magnitude softer than these fruits. The reported values for fruits are estimates of a healthy condition, and it is expected that they drastically decrease in fruits infested with fruit-fly larvae. Unfortunately, mechanical properties of the relevant decaying fruits are not known. It is thus impossible to determine whether the physical properties of the gels used in this study match those of the decaying fruit. Our estimation is that the gels represent such conditions reasonably well. Because we saw changes in probing kinematics in different gel densities, we hypothesize that wasps can adapt to different material properties in fruits.

Similar to increased substrate density, curving of the ovipositor also increased the amount of energy required for ovipositor insertion due to increased friction between the ovipositor and

the substrate. This explains the lower insertion speeds for curved parts of trajectories observed in our study. It also indicates that curving is an energetically expensive behavior that might be better avoided if possible.

We show that reciprocal valve movements are used when inserting slender probes into solid substrates. The estimated net forces acting on the valves are the first quantification of the push–pull mechanism in vivo. The low values are in agreement with the proposed insertion mechanism characterized by minimal net external pushing force. Furthermore, the relative position of the valves dictates the shape of the tip and influences the direction of probe insertion, probably by manipulating the size and direction of the substrate reaction forces. This improves the insight in the overall mechanism of oviposition in hymenopterans. Understanding of the mechanism will deepen the knowledge of adaptations in the ovipositor apparatus and the evolution of the taxon as a whole.

In addition, our findings can help advance the development of steerable man-made probes that is on the rise in the past decade (27, 62, 74) and is particularly relevant for the design of multielement probes (39, 40, 75). Miniaturization of the needle diameter should presumably be possible also for the needles used in solid substrates if the individual elements are operated in an alternating manner. The adjustable bevel shape, although already partially implemented (e.g., ref. 61), can be greatly enhanced by implementing pretension of the elements. Despite having multiple elements, the control of such needles may not necessarily be complicated, as it would be enough to monitor the juxtaposition of individual elements that would dictate the direction and amplitude of curving.

Materials and Methods

Substrate Properties. We used gellan gel, a microbial polysaccharide (76), as the probing substrate because of its translucency, isotropic properties, and readiness of the animals to insert their ovipositors in it. The rheological properties, namely, the storage (G') and loss (G'') moduli, of the gels used in the experiments were measured with a rotational rheometer (Anton Paar) and a cone plate probe (diameter of 25 mm) at 20°C. The gels were amorphous and considered isotropic (i.e., random cross-linking of hydrophilic polymer chains was assumed). To ensure a strong contact with the equipment, the gels were poured onto the base plate, and the probe was lowered into the gels while they were still warm. The gel was then left to cool down before starting the experiments. The linear strain region of the gel was obtained by first measuring the response to a changing strain (amplitude range: 0.1–100%) at a constant angular velocity (0.16 rad s^{-1}). Another gel of the same concentration was used for the measurements at a constant strain within the linear strain regime (0.2%) with a changing angular frequency of the probe (1–100 rad s^{-1}). The frequency measurements were repeated three times with 1-min intervals. The obtained moduli were averaged across repetitions and frequencies to calculate the dynamic shear modulus (G^*) and the dynamic elastic modulus (E^*). We assumed a Poisson's ratio (ν) of 0.5 because of the high water content of the gels. See *SI Materials and Methods* for details of the calculations.

Animals. Adult parasitic wasps (*D. longicaudata*) and their host, the Mediterranean fruit-fly *Ceratitis capitata*) were kept separately in rearing cages (30 × 30 × 30 cm, BugDorm; MegaView Science) at 24 °C and 12/12-h light/dark cycle, with ad libitum access to water and food. Wasp were fed commercially available honey, and flies were fed a mixture of glucose and brewer's yeast dissolved in tap water.

The flies could freely reproduce and lay their eggs in perforated plastic bottles. The eggs were harvested and put in oxygenated water for 1 d before transferring them to the larval medium, which was a mixture of brewer's yeast, carrot powder, sodium benzoate (food preservative), methylparaben (antifungal agent), hydrochloric acid (HCl; acidity regulator), and tap water. The larvae were exposed to parasitoids between the fourth and seventh day after hatching. After parasitation, the larvae were taken away from the wasps and left to develop and pupate in small boxes of vermiculite. After ∼2 wk, the wasps emerged from pupae of parasitized larvae. Fly larvae used for propagation of fly colonies were never exposed to parasitation and were kept apart from the wasps. For details of the rearing protocol, see *SI Materials and Methods*.

Experimental Setup and Data Acquisition. The 3D insertion path of the ovipositor in the substrate was recorded with two synchronized high-speed video cameras (Fastcam SA-X2; Photron) fitted with macro lenses (MP-E 65; Canon; 5× magnification factor) at 125 fps. The cameras' optical axes were perpendicular to each other (89 ± 1 °; Fig. 7*A*). Two near-collimated light beams were produced by using combinations of an approximate point light source and a 4-diopter lens, arranged in a backlight configuration. This resulted in a shadow image and a depth of focus of ∼1 mm. The cameras recorded probing events in a cuvette (inner dimensions 10.5 × 10.5 × 6 mm) with the probing medium in the center. A micromanipulator allowed translation of the cuvette in three directions to get the ovipositor within the field of view and the depth of field of the cameras. The cuvette was located in a closed-off glass arena (inner dimensions 48 × 48 × 48 mm).

Conversion of camera image pixels to the actual distances was done by using still images of copper specimen support grids for electron microscopy (0050-Cu; Electron Microscopy Sciences). The grid mesh size was measured with a calibrated microscope (Leica M205FA; Leica Microsystems; 20× magnification), after which the grids were put in a cuvette and embedded in the gel, which was also used in the experiments (see below). The difference in vertical position of the cameras was corrected based on the mean vertical coordinate (depth) of the most distal part of the tracked ovipositor tip in both camera views.

An additional camera (piA640-210-gm, 50 fps; Basler AG; with a Nikkor AF-50 lens; Nikon) recorded the spatial orientation of the probing wasp from above. The conversion from pixels to actual lengths for the images of this camera was calculated based on the known dimensions of the cuvette. Image time stamps were used to match the recordings between nonsynchronized cameras.

Probing behavior was recorded (Fig. 7*A*) in substrates with two different densities to assess the effect of substrate properties. The substrate contained commercially available apple juice (10%), tap water (90%), and gelling agent (Phytagel; Sigma-Aldrich) in either 0.02 g mL^{-1} (2%) or 0.04 g mL^{-1} (4%). The bottom of each cuvette contained a live, 4- to 7-d-old *C. capitata* larva and some of its rearing medium, covered with a fine cloth. A piece of wet filter paper with thinly spread larval medium was on the top of the substrate. The presence of these cues induced and prolonged the probing behaviors of the wasps. At the start of an experiment, several wasps were put in the arena, and nonresponsive females (i.e., those not motivated to probe) were removed until only one responsive animal was left. Upon initiation of probing, the position of the arena was manually adjusted to have the ovipositor in focus, after which no further adjustments were made to avoid movement artefacts. After a successful recording, wasps were isolated to ensure analysis of probing behavior of each animal in both 2% and 4% substrate. Each gel was used for several wasps until either the gel started showing signs of drying or the transparency reduced too much due to the number of probing paths.

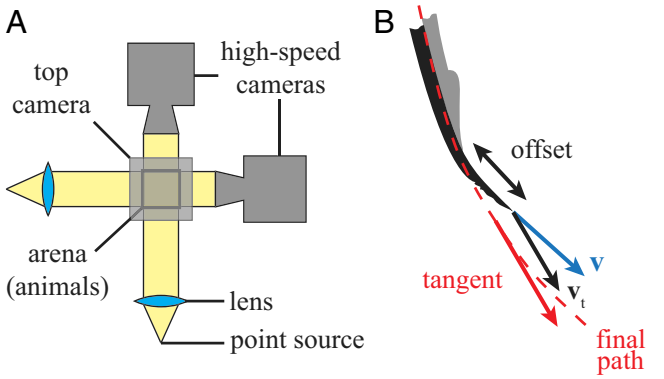

Fig. 7. Experimental setup and calculation of insertion speed. (*A*) Two high-speed cameras were positioned perpendicular to each other, each aligned with a near-collimated light beam (yellow). The arena with the substrate-filled cuvette and the animals was located in the field of view of both cameras. The third camera was located above the experimental arena, directed downward. (*B*) Schematics of the ovipositor during insertion in 2D (only two valves are shown). The tangential projection ($\mathbf{v_t}$) of the valve velocity ($\mathbf{v}$) along the final centerline (dashed, red line) was taken as the insertion speed. Insertion speed was calculated from the velocity of the foremost valve.

Data Analysis

Automatic Tracking. A single animal usually probed the substrate more than once. We defined all movements of the ovipositor made through a single puncture point of the surface as one insertion session. Such a session in general consisted of several insertions, which we defined as movement of the ovipositor into the substrate away from the puncture point. Image sequences of insertion sessions were split into individual insertions and cropped such that they contained only the full insertion trajectory.

In these image sequences, the ovipositors were segmented by using custom-built code in Matlab (Versions R2013a and R2016b; MathWorks). First, the background (average of first five frames of each insertion) was subtracted from all images. This was followed by a conversion to binary images based on a threshold adapted to each image sequence such that the ovipositor silhouette was clearly recognizable. Smaller objects and artefacts were removed by a dilation and erosion procedure, sometimes supplemented with manual input. This section of the ovipositor that was visible only in the first five frames had to be segmented from the background images separately and then combined with other images to obtain a complete trajectory. The segmentation of the ovipositor in the background images was done with ilastik (ilastik: Interactive Learning and Segmentation Toolkit; Version 1.1).

By using the cleared images, the centerline of the ovipositor in each frame was obtained by skeletonizing the segmented ovipositor and fitting a cubic smoothed spline curve through it (goodness of fit was determined by visual inspection). Because the tip of the skeletonized ovipositor was often irregular due to irregularities in the gel, the distal end of the skeleton was not used for fitting. The position of the most distal part of the ovipositor tip was determined by linear extrapolation of the centerline up to the boundary of the segmented ovipositor within $>7.5\,^{\circ}$.

Images from the top camera were cropped and converted to binary images based on thresholds adapted to the individual image sequence so that the silhouette of the animal was clearly recognizable. This was followed by morphological open and close operations to improve the segmentation. Ellipses were then fitted to segmented animals in each frame. The orientation (azimuth) of the animal was defined by the direction angle of the ellipse's major axis directed toward the animal's head with the Y axis of the world coordinate system (defined below).

The 3D probing trajectories were obtained by combining the two perpendicular coordinate systems of the cameras into a right-handed world coordinate system. The 3D trajectories were smoothed with a quintic spline function to ensure continuous second derivatives needed for calculating the curvature. All 3D trajectories were aligned such that the first insertion was set to the common origin $(0,0,0)$. The curves were then rotated around the Z axis to correct for the orientation of the animals so that the body axis was aligned with the positive Y axis. For each point of the trajectories, the amplitude of the curvature κ of the ovipositor was calculated by using the expression obtained from the general formula for a parametrically defined curve (77):

$$\kappa = \frac{\| \mathbf{l}(\mathrm{s})' \times \mathbf{l}(\mathrm{s})'' \|}{\| \mathbf{l}(\mathrm{s})' \|^3} = \sqrt{\frac{(y'z'' - y''z')^2 + (x''z' - x'z'')^2 + (x'y'' - x''y')^2}{(x'^2 + y'^2 + z'^2)^3}},$$

where $\mathbf{l}(\mathrm{s})$ is the vector function of the curve expressed as function of its arc length (s), and $'$ and $''$ denote the first and second derivatives with respect to the arc length. The dimensionless curvature was obtained by multiplying κ with the diameter of the ovipositor (30 μm, estimated from SEM images).

Probing velocity was calculated by taking the gradient of the filtered position data of the most distal part of the ovipositor tip (2^{nd} order low-pass Butterworth filter, cutoff frequency 15 Hz applied twice using Matlab "filtfilt" function, effectively using a 4^{th} order filter).

In the analysis of the 3D dataset, the insertion speed was taken as the magnitude of the component of the velocity vector tangential to the centerline of the final path at each time point (Fig. 7*B*). Retractions were not analyzed. The speed of the foremost valve was taken as the insertion speed of the entire ovipositor.

Analysis of valve kinematics in 2D was done for three insertion examples where individual valves were clearly in focus (see below). Valve insertion and retraction speeds were calculated as the magnitude of the components of the instantaneous velocity tangential to the instantaneous ovipositor centerline in each frame. We also discriminated between the speed of the dorsal and the foremost ventral valve.

Analysis of Valve Kinematics. The high magnification used, resulted in a narrow depth of field (DoF), which limited the tracking to a single camera view and to only parts of insertions. We chose image sequences where the ovipositor was moving within the plane of the DoF (i.e., did not curve in the view of the second camera). In our backlit images, only silhouettes of the valves were discernible, so only the most protruded (foremost) ventral valve could be recognized. The most distal ends of the dorsal and the foremost ventral valve tips were manually digitized in all frames where the ovipositor tip was in focus. The dorsal valve could easily be distinguished from the ventral valves based on its morphology (Fig. 1*A*).

The digitized points together with the frame-by-frame centerlines were used to calculate the tangential velocity of the valves as described above. In addition, the distance between the digitized most distal ends of the valve tips in each frame was taken as the offset between the valves. Positive offset denotes protraction of the dorsal valve, and negative denotes the protraction of the foremost ventral valve.

The ovipositor was segmented as described above, except for the example shown in Fig. 6*C*, which was done by using ilastik. In the latter example, the segmentation routine in Matlab yielded unsatisfactory results due to a complex background of the images. Automated tracking of the insertion was accurate, so there was no need to remove spurious ends of the skeletons and the extrapolation of the centerlines (as above).

Orientation of the ovipositor tip during insertion was calculated from the end part of the centerline. The length of the end part was taken as one-third of the length of the dorsal valve tip. We calculated the angle between the orientation of the ovipositor tip and the horizontal plane. We filtered the orientation data in time (2^{nd} order low-pass Butterworth filter, cutoff frequency 18.75 Hz applied twice using the Matlab filtfilt function), which reduced the frame to frame artefacts, but retained the overall temporal characteristics (Fig. S7 *A–C*). We then transformed the orientation data from the image frame of reference into the ovipositor frame of reference by subtracting the baseline orientation (2^{nd} order low-pass Butterworth filter, cutoff frequency 1 Hz applied twice by using the Matlab filtfilt function) from the direction data (Fig. S7 *D–F*).

The data are available on Dryad (http://dx.doi.org/10.5061/dryad.8bc95).

Estimating the Accelerations and the Net Forces on the Valves. The net forces on the valves (Figs. S3–S5) were estimated by taking the second derivative of the filtered position data, combined with a simplified cylindrical model of the ovipositor assuming simple material properties (Fig. S8). The density of the cuticle was taken from ref. 78. For details of force calculations see *SI Materials and Methods*.

ACKNOWLEDGMENTS. We thank Francisco Beitia (Instituto Valenciano de Investigaciones Agrarias) for providing parasitoids and Carlos Cáceres (International Atomic Energy Agency) for providing fruit-flies for our colony; Marleen Kamperman and Marco Dompé (Physical Chemistry and Soft Matter, Wageningen University and Research) for their assistance with the rheological measurements of the substrates; Henk Schipper, Remco Pieters, and Karen Leon-Kloosterziel for technical support and animal care; Cees Voesenek for advice on analytical methods; Dimitra Dodou (Delft University of Technology) for advice on the experiments; and the user committee of the Netherlands Organization for Scientific Research Division Applied and Engineering Sciences (NWO TTW) WASP project and the members of the research group for their useful discussions. This work was supported by NWO domain applied and engineering sciences (NWO TTW).

1. Le Lannic J, Nénon JP (1999) Functional morphology of the ovipositor in *Megarhyssa atrata* (Hymenoptera, Ichneumonidae) and its penetration into wood. *Zoomorphology* 119:73–79.
2. Ovruski S, Aluja M, Sivinski J, Wharton R (2000) Hymenopteran parasitoids on fruit-infesting Tephritidae (Diptera) in Latin America and the Southern United States: Diversity, distribution, taxonomic status and their use in fruit fly biological control. *Integrated Pest Manag Rev* 5:81–107.
3. Belshaw R, Grafen A, Quicke DLJ (2003) Inferring life history from ovipositor morphology in parasitoid wasps using phylogenetic regression and discriminant analysis. *Zoolog J Linn Soc* 139:213–228.
4. Smith EL (1970) Evolutionary morphology of the external insect genitalia. 2. Hymenoptera. *Ann Entomol Soc Am* 63:1–27.
5. Quicke DLJ, Fitton MG, Tunstead JR, Ingram SN, Gaitens PV (1994) Ovipositor structure and relationships within the Hymenoptera, with special reference to the Ichneumonoidea. *J Nat Hist* 28:635–682.
6. Ghara M, Kundanati L, Borges RM (2011) Nature's Swiss army knives: Ovipositor structure mirrors ecology in a multitrophic fig wasp community. *PLoS One* 6:e23642.
7. Schudder GGE (1961) The comparative morphology of the insect ovipositor. *Trans R Entomol Soc Lond* 113:2–40.
8. Lyngnes R (1960) Shape and function of the ovipositor in the three hymenopterous species: *Ephialtes extensor* Thom. (Ichneumonidae), *Spathius exarator* L. (Braconidae), and *Plutothrix coelius* walk. (Chalcididae). *Norsk Entomologisk Tidsskrift* 11:122–134.
9. King PE (1962) The muscular structure of the ovipositor and its mode of function in *Nasonia vitripennis* (Walker) (Hymenoptera: Pteromalidae). *Proc R Entomol Soc Lond Ser A Gen Entomol* 37:121–128.
10. Quicke DLJ (2015) *The Braconid and Ichenumonid Parasitoid Wasps: Biology, Systematics, Evolution and Ecology* (John Wiley & Sons, Ltd, Chichester, UK), 1st Ed, p 595.
11. Vilhelmsen L, Turrisi GF (2011) Per arborem ad astra: Morphological adaptations to exploiting the woody habitat in the early evolution of Hymenoptera. *Arthropod Struct Dev* 40:2–20.
12. Vilhelmsen L (2000) Before the wasp-waist: Comparative anatomy and phylogenetic implications of the skeleto-musculature of the thoraco-abdominal boundary region in basal Hymenoptera (Insecta). *Zoomorphology* 119:185–221.
13. Sharkey MJ (2007) Phylogeny and classification of Hymenoptera. *Zootaxa* 1668:e548.
14. Davis RB, Baldauf SL, Mayhew PJ (2010) The origins of species richness in the Hymenoptera: Insights from a family-level supertree. *BMC Evol Biol* 10:109.
15. Peters RS, et al. (2017) Evolutionary history of the Hymenoptera. *Curr Biol* 27: 1013–1018.
16. Matushkina N, Gorb S (2007) Mechanical properties of the endophytic ovipositor in damselflies (Zygoptera, Odonata) and their oviposition substrates. *Zoology (Jena)* 110:167–175.
17. Polidori C, García AJ, Nieves-Aldrey JL (2013) Breaking up the wall: Metal-enrichment in ovipositors, but not in mandibles, co-varies with substrate hardness in gall-wasps and their associates. *PLoS One* 8:e70529.
18. Kundanati L, Gundiah N (2014) Biomechanics of substrate boring by fig wasps. *J Exp Biol* 217:1946–1954.
19. Smith EL, Behavior O (1972) Biosystematics and morphology of Symphyta - III external genitalia of Euura (Hymenoptera: Tenthredinidae): Sclerites, sensilla, musculature, development and oviposition behaviour. *Int J Insect Morphol Embryol* 1:321–365.
20. Field SA, Austin AD (1994) Anatomy and mechanics of the telescopic ovipositor system of *Scelio latreille* (Hymenoptera: Scelionidae) and related genera. *Int J Insect Morphol Embryol* 23:135–158.
21. Vilhelmsen L, Isidoro N, Romani R, Basibuyuk HH, Quicke DLJ (2001) Host location and oviposition in a basal group of parasitic wasps: The subgenual organ, ovipositor apparatus and associated structures in the Orussidae (Hymenoptera, Insecta). *Zoomorphology* 121:63–84.
22. Heatwole H, Davis DM, Wenner AM (1962) The behaviour of Megarhyssa, a genus of parasitic hymenopterans (Ichneumonidae: Ephialtinae). *Z Tierpsychol* 19:652–664.
23. Vincent JFV, King MJ (1995) The mechanism of drilling by wood wasp ovipositors. *Biomimetics* 3:187–201.
24. Vilhelmsen L (2003) Flexible ovipositor sheaths in parasitoid Hymenoptera (Insecta). *Arthropod Struct Dev* 32:277–287.
25. Elias LG, Teixeira SP, Kjellberg F, Santinelo Pereira RA (2012) Diversification in the use of resources by *Idarnes* species: Bypassing functional constraints in the fig-fig wasp interaction. *Biol J Linn Soc* 106:114–122.
26. Abolhassani N, Patel R, Moallem M (2007) Needle insertion into soft tissue: A survey. *Med Eng Phys* 29:413–431.
27. Misra S, Reed KB, Douglas AS, Ramesh KT, Okamura AM (2008) Needle-Tissue interaction forces for bevel-tip steerable needles. *Proc Biennial IEEE/RAS-EMBS Int Conf Biomed Robot Biomechatron* 2:224–231.
28. Abayazid M, Roesthuis RJ, Reilink R, Misra S (2013) Integrating deflection models and image feedback for real-time flexible needle steering. *IEEE Trans Robotics* 29: 542–553.
29. Le Ralec A, Rabasse JM, Wajnberg E (1996) Comparative morphology of the ovipositor of some parasitic Hymenoptera in relation to characteristics of their hosts. *Can Entomol* 128:413–433.
30. Gerling D, Quicke DLJ, Orion T (1998) Oviposition mechanisms in the whitefly parasitoids *Encarsia transvena* and *Eretmocerus mundus*. *BioControl* 43:289–297.
31. Ko SY, Frasson L, Baena FRY (2011) Closed-loop planar motion control of a steerable probe with a "programmable bevel" inspired by nature. *IEEE Trans Robot* 27:970–983.
32. Quicke DLJ, Fitton M, Harris J (1995) Ovipositor steering mechanisms in braconid wasps. *J Hymenoptera Res* 4:110–120.
33. Quicke DLJ, Fitton MG (1995) Ovipositor steering mechanisms in parasitic wasps of the families Gasteruptiidae and Aulacidae (Hymenoptera). *Proc R Soc Biol Sci* 261:98–103.
34. Quicke DLJ (1991) Ovipositor mechanics of the braconine wasp genus *Zaglyptogastra* and the ichneumonid genus *Pristomerus*. *J Nat Hist* 25:971–977.
35. Pollard DG (1969) Directional control of the stylets in phytophagous Hemiptera. *Proc R Entomol Soc Lond Ser A Gen Entomol* 44:173–185.
36. Pollard DG (1971) The use of polyporus for the investigation of stylet behaviour in the Hemiptera. *Entomol Exp Appl* 14:283–296.
37. Compton S, Nefdt R (1988) Extra-long ovipositors in chalcid wasps: Some examples and observations. *J Antenn* 12:102–105.
38. Sears P, Dupont P (2006) A steerable needle technology using curved concentric tubes. Proceedings of the 2006 IEEE/RSJ International Conference on Intelligent Robots and Systems, Beijing *(IEEE, Piscataway, NJ), pp* 2850–2856.
39. Parittotokkaporn T, et al. (2009) Soft tissue traversal with zero net force: Feasibility study of a biologically inspired design based on reciprocal motion. Proceedings of the 2008 IEEE International Conference on Robotics and Biomimetics, Bangkok *(IEEE, Piscataway, NJ),* pp 80–85.
40. Frasson L, et al. (2010) STING: A soft-tissue intervention and neurosurgical guide to access deep brain lesions through curved trajectories. *Proc IME H J Eng Med* 224: 775–788.
41. Roesthuis RJ, van Veen YR, Jahya A, Misra S (2011) Mechanics of needle-tissue interaction. *Proceedings of the Proceedings of the 2011 IEEE/RSJ International Conference on Intelligent Robots and Systems, San Francisco* (IEEE, Piscataway, NJ), pp 2557–2563.
42. Ko SY, Baena RYF (2012) Trajectory following for a flexible probe with state/input constraints: An approach based on model predictive control. *Robot Autonom Syst* 60:509–521.
43. Elgezua I, Kobayashi Y, Fujie MG (2013) Survey on current state-of-the-art in needle insertion robots: Open challenges for application in real surgery. *Proced CIRP* 5:94–99.
44. Consoli FL, Kitajima EW, Postali Parra JR (1999) Sensilla on the antenna and ovipositor of the parasitic wasps *Trichogramma galloi* Zucchi and *T. pretiosum* Riley. *Microsc Res Tech* 45:313–324.
45. Hawke SD, Farley RD, Greany PD (1973) The fine structure of sense organs in the ovipositor of the parasitic wasp, *Orgilus lepidus* Muesebeck. *Tissue Cell* 5:171–184.
46. van Lenteren JC, et al. (2007) Structure and electrophysiological responses of gustatory organs on the ovipositor of the parasitoid *Leptopilina heterotoma*. *Arthropod Struct Dev* 36:271–276.
47. Shah ZA (2012) Morphology, ultrastructure, and probable functions of the sense organs on the ovipositor stylets of the hymenoptran parasitoid, *Venturia canescens* (Gravenhorst). *Microsc Res Tech* 75:876–883.
48. van Lentern JC, et al. (1998) Functional anatomy of the ovipositor clip in the parasitoid *Leptopilina heterotoma* (Thompson) (Hymenoptera: Eucolidae), a structure to grip escaping host larvae. *Int J Insect Morphol Embryol* 27:263–268.
49. Vinson SB (1976) Host selection by insect parasitoids. *Annu Rev Entomol* 21:109–133.
50. Spradbery JP (1970) Host finding by *Rhyssa persuasoria* (L.) in ichneumonid parasite of siricid woodwasps. *Anim Behav* 18:103–114.
51. Ghara M, Ranganathan Y, Krishnan A, Gowda V, Borges RM (2014) Divvying up an incubator: How parasitic and mutualistic fig wasps use space within their nursery microcosm. *Arthropod Plant Interact* 8:191–203.
52. Kim BH, Kim HK, Lee SJ (2011) Experimental analysis of the blood-sucking mechanism of female mosquitoes. *J Exp Biol* 214:1163–1169.
53. Gordon RM, Lumsden WHR (1939) A study of the behaviour of the mouth-parts of mosquitoes when taking up blood from living tissue together with some observations on the ingestion of microfilariae. *Ann Trop Med Parasitol* 33:259–278.
54. Griffiths RB, Gordon RM (1952) An apparatus which enables the process of feeding by mosquitoes to be observed in the tissues of a live rodent; together with an account of the ejection of saliva and its significance in malaria. *Ann Trop Med Parasitol* 46: 311–319.
55. Kong X, Wu C (2009) Measurement and prediction of insertion force for the mosquito fascicle penetrating into human skin. *J Bionic Eng* 6:143–152.
56. Choumet V, et al. (2012) Visualizing non infectious and infectious *Anopheles gambiae* blood feedings in naive and saliva-immunized mice. *PLoS One* 7:e50464.
57. Kong XQ, Wu CW (2010) Mosquito proboscis: An elegant biomicroelectromechanical system. *Phys Rev E Stat Nonlin Soft Matter Phys* 82:011910.

58. Izumi H, et al. (2008) Combined harpoonlike jagged microneedles imitating mosquito's proboscis and its insertion experiment with vibration. *IEEJ Trans Electr Electron Eng* 3:425–431.
59. Freeman TP, Buckner JS, Nelson DR, Chu CC, Henneberry TJ (2001) Stylet penetration by *Bemisia argentifolii* (Homoptera: Aleyrodidae) into host leaf tissue. *Ann Entomol Soc America* 94:761–768.
60. Leopold RA, Freeman TP, Buckner JS, Nelson DR (2003) Mouthpart morphology and stylet penetration of host plants by the glassy-winged sharpshooter, *Homalodisca coagulata* (Homoptera: Cicadellidae). *Arthropod Struct Dev* 32:189–199.
61. Frasson L, Ferroni F, Ko SY, Dogangil G, Baena RYF (2011) Experimental evaluation of a novel steerable probe with a programmable bevel tip inspired by nature. *J Robot Surg* 6:189–197.
62. Webster IIIRJ, Kim JS, Cowan NJ, Chirikjian GS, Okamura AM (2006) Nonholonomic modeling of needle steering. *Int J Robot Res* 25:509–525.
63. Dai W, Pan L, Lu Y, Jin L, Zhang C (2014) External morphology of the mouthparts of the whitebacked planthopper *Sogatella furcifera* (Hemiptera: Delphacidae), with special reference to the sensilla. *Micron* 56:8–16.
64. Zhao L, Dai W, Zhang C, Zhang Y (2010) Morphological characterization of the mouthparts of the vector leafhopper *Psammotettix striatus* (L.) (Hemiptera: Cicadellidae). *Micron* 41:754–759.
65. Kang KS, Veeder GT, Mirrasoul PJ, Kaneko T, Cottrell IW (1982) Agar-like polysaccharide produced by a *Pseudomonas* species: Production and basic properties. *Appl Environ Microbiol* 43:1086–1091.
66. Nussinovitch AMMA, et al. (1990) Characterization of gellan gels by uniaxial compression, stress relaxation and creep. *J Texture Stud* 21:37–50.
67. Finney EEJ (1967) Dynamic elastic properties of some fruits during growth and development. *J Agric Eng Res* 12:249–256.
68. Leyva JL, Browning HW, Gilstrap FE (1991) Effect of host fruit species, size, and color on parasitization of *Anastrepha ludens* (Diptera: Tephritidae) by *Diachasmimorpha longicaudata* (Hymenoptera: Braconidae). *Environ Entomol* 20:1469–1474.
69. Segura DF, Nussenbaum AL, Viscarret MM (2016) Innate host habitat preference in the parasitoid *Diachasmimorpha longicaudata*: Functional significance and modifications through learning. *PLoS One* 11:e0152222.
70. Fridley RB, Bradley RA, Rumsey JW, Adrian PA (1968) Some aspects of elastic behavior of selected fruits. *Trans Am Soc Agric Eng* 11:46–49.
71. Delwiche MJ, McDonald T, Bowers SV (1987) Determination of peach firmness by analysis of impact forces. *Trans Am Soc Agric Eng* 30:249–254.
72. Fidelibus MW, Teixeira AA, Davies FS (2002) Mechanical properties of orange peel and fruit treated pre-harvest with gibberellic acid. *Trans Am Soc Agric Eng* 45:1057–1062.
73. Singh KK, Reddy BS (2006) Post-harvest physico-mechanical properties of orange peel and fruit. *J Food Eng* 73:112–120.
74. Misra S, Reed KB, Schafer BW, Ramesh KT, Okamura AM (2010) Mechanics of flexible needles robotically steered through soft tissue. *Int J Robot Res* 29:1640–1660.
75. Ko SY, Davies BL, Baena RYF (2010) Two-dimensional needle steering with a "programmable bevel" inspired by nature: Modeling preliminaries. *2010 IEEE/RSJ Int Conf Intell Robots Syst* 2319–2324.
76. Jansson PE, Bengt L (1983) Structural studies of gellan gum, an extracellular polysaccharide elaborated by Pseudomonas elodea. *Carbohydr Res* 124:135–139.
77. O'Neal B (1966) *Elementary Differential Geometry*, ed O'Neal B (Academic, London), 1st Ed, p 422.
78. Vincent JFV, Wegst UGK (2004) Design and mechanical properties of insect cuticle. *Arthropod Struct Dev* 33:187–199.